



**HAL**  
open science

## Dynamic Flux Balance Analysis of the Metabolism of Microalgae under a Diurnal Light Cycle

Caroline Baroukh, Jean Philippe Steyer, Olivier Bernard, Benoit Chachuat

► **To cite this version:**

Caroline Baroukh, Jean Philippe Steyer, Olivier Bernard, Benoit Chachuat. Dynamic Flux Balance Analysis of the Metabolism of Microalgae under a Diurnal Light Cycle. DYCOPS-CAB 2016 - 11th IFAC Symposium on Dynamics and Control of Process Systems, Including Biosystems DYCOPS-CAB 2016, International Federation of Automatic Control (IFAC). AUT., Jun 2016, Trondheim, Norway. pp.791 - 796, 10.1016/j.ifacol.2016.07.285 . hal-01413531

**HAL Id: hal-01413531**

**<https://inria.hal.science/hal-01413531>**

Submitted on 3 Jun 2020

**HAL** is a multi-disciplinary open access archive for the deposit and dissemination of scientific research documents, whether they are published or not. The documents may come from teaching and research institutions in France or abroad, or from public or private research centers.

L'archive ouverte pluridisciplinaire **HAL**, est destinée au dépôt et à la diffusion de documents scientifiques de niveau recherche, publiés ou non, émanant des établissements d'enseignement et de recherche français ou étrangers, des laboratoires publics ou privés.

## dynamic Flux Balance Analysis of the Metabolism of Microalgae under a Diurnal Light Cycle

C. Baroukh<sup>\*,†,‡</sup>, JP Steyer<sup>\*</sup>, O. Bernard<sup>‡</sup>  
B. Chachuat<sup>†</sup>

<sup>\*</sup>INRA, UR0050 Laboratoire de Biotechnologie de l'Environnement, F-11100 Narbonne  
FRANCE (Tel: +33468425151; e-mail: caroline.baroukh@supagro.inra.fr).

<sup>†</sup> Centre for Process Systems Engineering, Department of Chemical Engineering, Imperial College London, South Kensington  
Campus, London SW7 2AZ, UNITED KINGDOM (e-mail: b.chachuat@imperial.ac.uk)

<sup>‡</sup> INRIA-BIOCORE, 2004 route des Lucioles, 06250 Sophia-Antipolis, FRANCE, (e-mail: olivier.bernard@inria.fr)

**Abstract:** Microalgae have received much attention in the context of renewable fuel production, due to their ability to produce in high quantities carbon storage molecules such as lipids and carbohydrates. Despite significant research effort over the last decade, the production yields remain low and need to be optimized. For that, a thorough understanding of carbon storage metabolism is necessary. This paper develops a constrained metabolic model based on the dFBA framework to represent the dynamics of carbon storage in microalgae under a diurnal light cycle. The main assumption here is that microalgae adapt their metabolism in order to optimize their production of functional biomass (proteins, membrane lipids, DNA, RNA) over a diurnal cycle. A generic metabolic network comprised of 160 reactions representing the main carbon and nitrogen pathways of microalgae is used to characterize the metabolism. The optimization problem is simplified by exploiting the right kernel of the stoichiometric matrix, and transformed into a linear program by discretizing the differential equations using a classical collocation technique. Several constraints are investigated. The results suggest that the experimentally observed strategy of accumulation of carbon storage molecules during the day, followed by their depletion during the night may indeed be the optimal one. However, a constraint on the maximal synthesis rate of functional biomass must be added for consistency with the biological observations.

**Keywords:** Microalgae; Dynamic modelling; dFBA; Metabolism; Photosynthesis; Carbon storage

### 1. INTRODUCTION

Microalgae are promising organisms in the context of renewable energy since they can grow using light and CO<sub>2</sub> and can store large quantities of lipids and carbohydrates (Mata et al. 2010), which can be converted into biofuels. Despite significant research effort over the last decade, the production yields remain low and need to be further optimized. For that, a thorough understanding of carbon storage metabolism is necessary, which could be achieved using systems biology and metabolic modelling. Indeed, *in silico* studies of microbial metabolism can help clarify the intracellular mechanisms and identify routes for enhancing the production of certain targeted molecules. There are many examples of successful optimization guided by metabolic modelling (Hamilton & Reed 2013), such as the *in silico* study of *Saccharomyces cerevisiae* metabolism that led to an increase of up to 25% in the production yield of ethanol on xylose/ glucose mixtures (Bro et al. 2006).

To understand carbon storage metabolism, it is important to study why such storage exists in the first place. For that, one needs to consider microalgae in the context of their natural habitats. Microalgae either grow in oceans (marine type) or lakes (freshwater type), where the culture media are usually limited by nutrient availability and subject to diurnal cycles. Because sunlight is the primary energy source in microalgae,

and energy is required for inorganic carbon assimilation, energy and carbon storage during the day appears to be a necessary strategy to meet the maintenance requirements during the night. Such an accumulation of lipids, carbohydrates or other carbon storage molecules during the day and their subsequent depletion during the night have been observed experimentally in several microalgae species (Knoop et al. 2013; Lacour et al. 2012). However, it has not been proved (or disproved) so far that this strategy is optimal under a diurnal light cycle. In addition, the amount of carbon stored, its storage form (as carbohydrates, lipids, cyanophycin, glycerol, etc) and its accumulation/depletion kinetics are still not fully understood. In order to provide hints for answering such questions, this paper develops an optimization-based model capable of describing the metabolic behaviour of a generic microalgae species under a diurnal light cycle. This model relies on dynamic Flux Balance Analysis (dFBA) (Mahadevan et al. 2002) and uses dynamic optimization. The paper is structured as follows: in section 2, the construction of the model is described, composed of i) metabolic network reconstruction, ii) adaptation of dynamic Flux Balance Analysis in the case of microalgae, iii) model formulation iv) simplification and linearization of the problem and v) numerical solution procedure. Then, in section 3, the model is solved and simulated. Several constraints are investigated and results are discussed and compared to experimental data.

## 2. MODEL FORMULATION

### 2.1 Metabolic network

The core carbon and nitrogen metabolic network among the microalgae species whose metabolic network has been reconstructed so far is relatively well conserved (Baroukh et al. 2015a). Here, we use a core metabolic network comprised of 160 reactions, which includes the following metabolic pathways relevant to autotrophy: photophosphorylation, Calvin cycle, pentose phosphate pathway, glycolysis, TCA cycle, oxidative phosphorylation, and synthesis of carbohydrates, lipids, amino acids, nucleotides and chlorophyll. Species-specific pathways, such as the synthesis of secondary metabolites, are not represented since the corresponding fluxes are usually negligible compared with the main pathways, and thus have a small impact on the metabolism. Then, the reactions of macromolecules synthesis (proteins, lipids, DNA, RNA and biomass) are lumped into generic reactions in order to arrive at a rather generic model, which is likely to describe a broad range of microalgae species (Baroukh et al., 2015b). The complete list of reactions and metabolites is available in the supplementary information of Baroukh et al. (2014).

### 2.2 dynamic Flux Balance Analysis

#### 2.2.1 Adaptation of the framework to represent accumulation of some metabolites

Dynamic Flux Balance Analysis (dFBA) (Mahadevan et al. 2002) is the dynamical extension of Flux Balance Analysis (Orth et al. 2010) for describing the metabolic behaviour of an organism. This framework relies on a quasi-steady state approximation (QSSA), which assumes no accumulation or depletion of intracellular metabolites. In order to represent carbon storage under the form of some intracellular metabolites, we represent the corresponding metabolites as external metabolites here, which are either excreted as products by the cell, or consumed as substrates within the cell. These metabolites are assumed to play no further functional role in the cell besides acting as storage (or buffers).

There are thus two types of intracellular metabolites inside the cell (Fig 1): *i*) those assumed to follow a QSSA (denoted by C), consumed as they are produced ( $\frac{dC}{dt} = 0$ ) for synthesizing new functional biomass (proteins, DNA, RNA, membrane carbohydrates and lipids); and *ii*) those assumed to act as carbon storage units (denoted by A), which are not consumed at the same time they are produced. Biomass *X* is thus divided into two pools: metabolites *A* and functional biomass *B*.

#### 2.2.2 Optimization problem formulation

Maximization of the production of biomass (B) over a 24h day/night cycle is chosen as objective function (1.1). The only model input is light (1.8), as all the other nutrients are assumed to be non-limiting. An additional constraint on the quota of *A* is added to ensure the cyclic behaviour of the

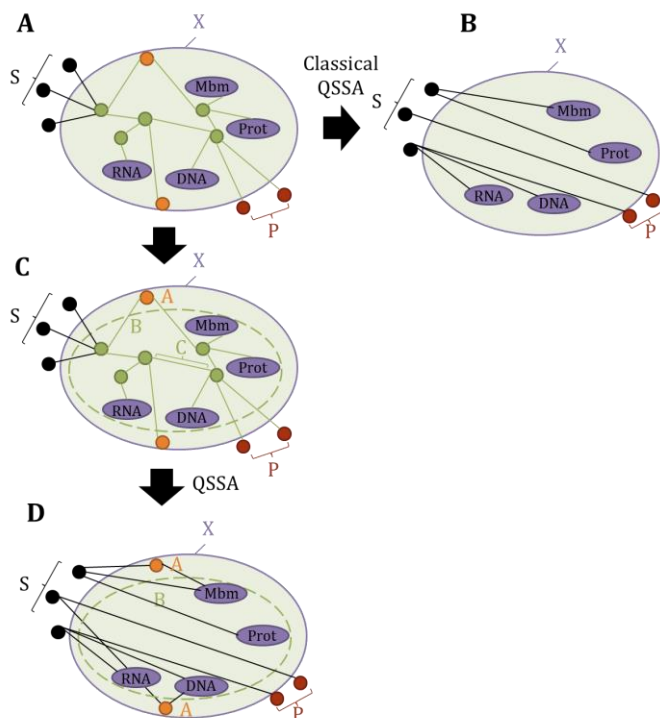


Fig. 1. Adaptation of dFBA taking carbon storage into account:

A. Schematic view of an organism metabolism, in which substrates (S) are converted, via intermediates metabolites (green and orange dots), into products (P) or biomass (X) (mainly composed of proteins (Prot), DNA, RNA, membrane carbohydrates and lipids (Mbm)).

B. Schematic view of an organism metabolism after application of classical QSSA (no accumulation of intracellular metabolites). Substrates (S) are directly converted into products (P) or biomass (X).

C. Schematic view of an organism metabolism, accounting for carbon storage. There are two types of intracellular metabolites: *i*) those assumed to follow a QSSA (C, green dots); and *ii*) those assumed to act as carbon storage units (A, orange dots). Biomass *X* is thus divided into two pools: metabolites *A* and functional biomass *B* – mainly composed of proteins (Prot), DNA, RNA, membrane carbohydrates and lipids (Mbm).

D. Schematic view of an organism metabolism after application of QSSA, when taking into account carbon storage. Substrates (S) are directly converted into products (P), functional biomass (B) or indirectly converted into products (P), functional biomass (B) via carbon storage metabolites (A).

metabolism (1.9), along with an optional constraint on the maximal kinetic rate (1.7). A formulation of dFBA optimization problem is as follows:

$$\max_{v(t)} \int_0^{24} B(t) dt \quad (1.1)$$

subject to

$$\frac{dM}{dt} = \frac{d(S)}{dt} = K \cdot v(t) \cdot B(t) = \begin{pmatrix} K_S \\ K_A \\ K_B \end{pmatrix} \cdot v(t) \cdot B(t) \quad (1.2)$$

$$M(0) = M_0 \quad (1.3)$$

$$M \geq 0 \quad (1.4)$$

$$K_C \cdot v(t) = 0 \quad (1.5)$$

$$v_i \geq 0 \text{ for } i \in Irr \quad (1.6)$$

$$v_j \leq v_{max} \text{ for some } j \in \{1, \dots, n_v\} \text{ (optional)} \quad (1.7)$$

$$v_l = effmax.I(t) \quad (1.8)$$

$$qA(24h) = \frac{A(24h)}{B(24h)} = \frac{A(0)}{B(0)} = qA(0) \quad (1.9)$$

with:

i)  $M$ , the vector of external metabolite concentrations of size  $n_M$  composed of substrates  $S$ , carbon storage metabolites  $A$  and biomass  $B$ ;

ii)  $M_0$ , the initial concentrations of the metabolites  $M$ ;

iii)  $K$  and  $K_C$ , the lines of the stoichiometric matrix of the metabolic network corresponding, respectively, to  $M$  and the intracellular metabolites;

iv)  $v$ , the kinetic rate vector of the  $n_v$  reactions;

v)  $Irr \subset \{1, \dots, n_v\}$ , the index subset of irreversible reactions;

vi)  $v_{max}$ , the maximal admissible kinetic rates of certain reactions;

vii)  $effmax$ , the conversion efficiency of the light input parameter ( $I(t)$ ) into energy for the reaction of the light phase of photosynthesis ( $v_l$ ); and

viii)  $q_A$  the biomass quota of  $A$ .

## 2.3 Simplification and linearization of the problem

### 2.3.1 Coordinate transform

Solving the optimization problem (1), involves identifying the 160 fluxes  $v(t)$ . In order to linearize the problem, we optimize for the transformed variables  $v' = v \cdot B$  instead of  $v$ . Then, by exploiting the right kernel ( $K_C \cdot Ker(K_C) = 0$ ) of the stoichiometric matrix  $K_C$ , the optimization problem simplifies to:

$$\max_{u(t)} \int_0^{24} B(t) dt \quad (2.1)$$

subject to

$$\frac{dM}{dt} = \frac{d \begin{pmatrix} S \\ A \\ B \end{pmatrix}}{dt} = K' \cdot u(t) \text{ with } K' = \begin{pmatrix} K_S \\ K_A \\ K_B \end{pmatrix} \cdot Ker(K_C) \quad (2.2)$$

$$M(0) = M_0 \quad (2.3)$$

$$M \geq 0 \quad (2.4) \quad (2)$$

$$Ker(K_C)_i \cdot u \geq 0 \text{ for } i \in Irr \quad (2.5)$$

$$Ker(K_C)_j \cdot u \leq v_{max} \cdot B \text{ for some } j \in \{1, \dots, n_v\} \text{ (optional)} \quad (2.6)$$

$$Ker(K_C)_l \cdot u = effmax.I(t) \cdot B(t) \quad (2.7)$$

$$qA(24h) = \frac{A(24h)}{B(24h)} = \frac{A(0)}{B(0)} = qA(0) \quad (2.8)$$

where  $v' = Ker(K_C) \cdot u$ , with  $u \in R^{11}$ . Note that the QSSA constraint (1.5) no longer appears in the optimization problem since it is satisfied by  $u$  construction.

### 2.3.2 Discretization

The optimization problem (2) is solved numerically by applying a discretization in the time domain, following a standard orthogonal collocation approach (Biegler 2010). The time interval  $[0;24h]$  is divided into  $N$  equally sized intervals, each of length  $h = \frac{24h}{N}$ . Each time interval contains  $K$  collocation points  $r_q \in [0;1]$ ,  $q \in \{1; \dots; K\}$ ,  $r_q$  chosen as the zeros of the Legendre polynomial of degree  $K$  here. The flux variable  $u(t)$  and time derivatives of the metabolite concentrations  $\frac{dM(t)}{dt}$  are discretized according to a Lagrange interpolation scheme:

$$u(t) = \sum_{q=1}^K u_{i,q} \cdot L_q\left(\frac{t-t_{i-1}}{h}\right), t_{i-1} \leq t \leq t_i, i = 1..N \quad (3)$$

$$\frac{dM(t)}{dt} = \sum_{q=1}^K \frac{dM}{dt}_{i,q} \cdot L_q\left(\frac{t-t_{i-1}}{h}\right), t_{i-1} \leq t \leq t_i, i = 1..N \quad (4)$$

with  $L_q, q = 1..K$  the Lagrange polynomials:

$$L_q(r) = \prod_{\substack{l=1 \\ l \neq q}}^K \frac{r-r_l}{r_q-r_l} \quad (5)$$

and  $t_i = i * h, i = 0,1, \dots, N$  the end-points of the time subintervals.

The metabolites' concentration vector  $M$  is discretized at each time interval and computed within each time interval by integrating the vector  $\frac{dM(t)}{dt}$ :

$$M(t) = M_{i-1} + h \cdot \sum_{q=1}^K \frac{dM}{dt}_{i,q} \int_0^{\frac{t-t_{i-1}}{h}} L_q(s) ds, \quad t_{i-1} \leq t \leq t_i, i = 1..N \quad (6)$$

The continuity of the concentrations  $M$  is enforced by the constraints:

$$M_i = M_{i-1} + h \cdot \sum_{q=1}^K \frac{dM}{dt}_{i,q} \int_0^1 L_q(s) ds, i = 1..(N-1) \quad (7)$$

Using this discretization scheme, the optimal control problem (2) is thus approximated by a linear program (LP) of the form:

$$f^* = \min_x f^T x \text{ s.t.} \quad (8)$$

$$A_{eq} x = b_{eq}$$

$$Ax \leq b$$

with

$$x = \left( M_0 \dots M_{N-1} \frac{dM}{dt}_{1,1} \dots \frac{dM}{dt}_{N,K} u_{1,1} \dots u_{N,K} \right)^T, \quad (9)$$

$$x \in \mathbb{R}^{(n_M \cdot N + n_M \cdot N \cdot K + n_U \cdot N \cdot K)}$$

where  $M_{i-1}$ ,  $\frac{dM}{dt}_{i,q}$  and  $u_{i,q}$ ,  $i = 1..N, q = 1..K$  correspond to the collocation coefficients in (3), (4) and (6).

## 2.4 Numerical solution procedure

The linear optimization problems (8) is solved using the LP solver Gurobi in Matlab, with the discretization parameters  $N=48$  and  $K=3$ . Initial values for the concentrations  $M$  and the discretized light intensity input parameter  $I(t)$  are taken from Lacour et al. (2012). Moreover, the parameter  $\text{effmax}$  is estimated to be  $0.0115 \text{ mM} \cdot \text{h}^{-1} \cdot \text{mMB}^{-1} \cdot \mu\text{E} \cdot \text{m}^{-2} \cdot \text{s}^{-1}$  in order to match the experimental observation of roughly a doubling time in 24h. Finally, carbon storage (A) is assumed to be only in the form of carbohydrates (CARB) here. A schematic representation of these assumptions is shown in Fig 2.

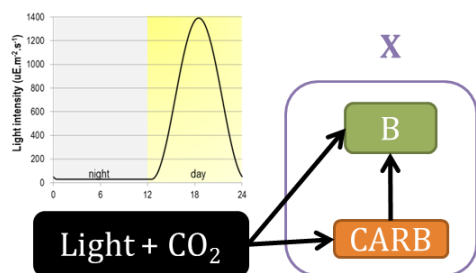


Fig. 2. A schematic view of the model.  $\text{CO}_2$  assimilation is driven by light energy. This available carbon is then converted via the metabolic network into carbohydrates (CARB) and biomass (B). CARB can also synthesize B. Total biomass  $X$  is composed of B and CARB. Light intensity follows a representative day/night cycle at Narbonne, France during summer (Lacour et al. 2012).

### 3. NUMERICAL RESULTS AND DISCUSSIONS

#### 3.1 Without constraint on $v_{max}$

A first case study is conducted by solving (8) without any constraint (2.6) on  $v_{max}$ . This model predicts an instantaneous consumption of CARB during the first time step ( $t=0.11\text{h}$ ), which leads to an instantaneous synthesis of B (Fig 3A-B). After this, both CARB and B stay constant during the rest of the dark period. During day time (from  $t=12\text{h}$  to  $24\text{h}$ ), light then allows to replenish the CARB pool, so as to satisfy the periodicity constraint (2.8) on metabolite storage. The CARB minimal carbon quota is about 17%, a value determined by the maximal light intensity during the day—the availability of light during the day determines how much energy can be produced, and therefore how much  $\text{CO}_2$  can be assimilated and how much CARB can be synthesized. If maximal light intensity increases to  $1800 \mu\text{E} \cdot \text{m}^{-2} \cdot \text{s}^{-1}$  (instead of  $1400 \mu\text{E} \cdot \text{m}^{-2} \cdot \text{s}^{-1}$ ), the CARB minimal quota drops to 0%, suggesting that the amount of carbon stored during the day is indeed related to the maximal light intensity.

A sharp decrease in the concentration  $X$  of the total carbon biomass is also observed during the first time step (Fig 3C). This is due to the fact that synthesis of B from CARB implies a release of  $\text{CO}_2$  by the TCA cycle, which is coupled with oxidative phosphorylation to meet the energy demand (under the form of ATP) in the absence of light. Then,  $X$  remains constant until day time, since CARB is no longer consumed and B is no longer produced. During day time,  $X$  increases because of CARB synthesis from light and  $\text{CO}_2$ . We note that

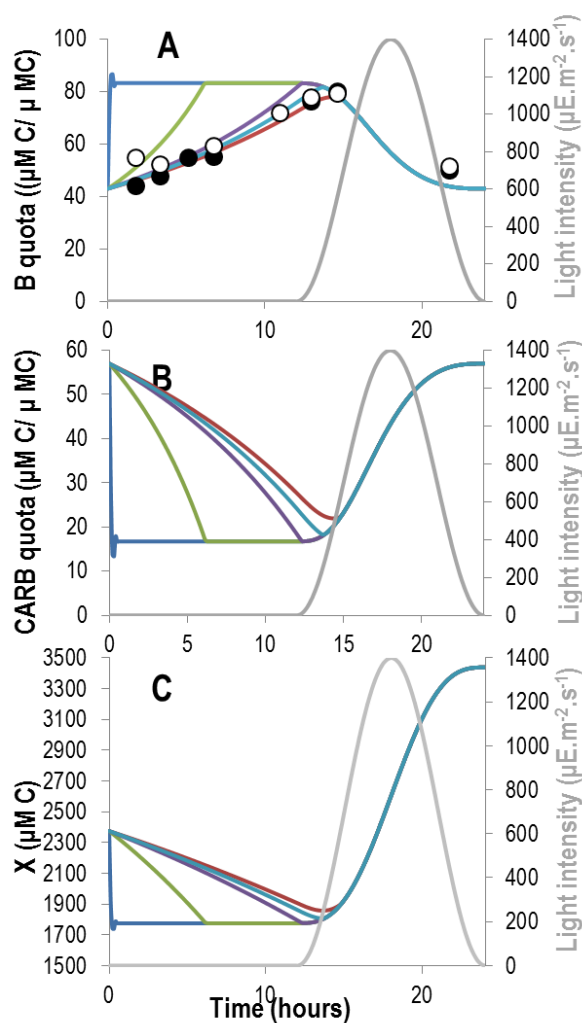


Fig. 3. Simulation results for several constraints  
Grey: Light intensity. Dark blue: without constraint on  $v_{max}$ . Others: with onstraints ( $\mu\text{M} \cdot \text{h}^{-1} \cdot \mu\text{MB}^{-1}$ ) on the biomass synthesis rate  $v_B$  (Green: 0.06, Purple: 0.03, Light blue: 0.028, Red: 0.025)  
A. Biomass (B) carbon quota. Dots: experimental data from Lacour et al. (2012) from duplicates.  
B. Carbohydrates (CARB) carbon quota.  
C. Total carbon biomass  $X$ .

the biomass  $X$  nearly doubles over a 24h period, in agreement with the experimental data by Lacour et al. (2012).

#### 3.2 With constraints on the biomass synthesis rate $v_B$

A second case study is conducted by solving (8) with a constraint on the maximal synthesis rate  $v_B$  of the biomass B. Several values of  $v_B$  lead to different behaviours of the system during night time (Fig 3), and to different optimal values of the cost function (Table 1) in turn. No difference in behaviour is observed during day time, on the other hand.

For values of  $v_B$  larger than  $0.03 \mu\text{M} \cdot \text{h}^{-1} \cdot \mu\text{MB}^{-1}$  (Fig 3 green and purple curves), CARB are no longer consumed instantaneously (Fig 3A), which shows that the maximal rate constraints are limiting (active) in the LP problem. CARB

reach their minimal quota values (and B their maximal quota values) before the end of dark period (Fig 3 A-B). These values are the same as those obtained without maximal rate constraints (Section 3.1). Once these quotas are reached, CARB and B stay constant until day time; then, light replenishes the CARB pool in order to satisfy the periodicity constraint (2.8). The variations in total carbon biomass  $X$  are also consistent with the conversion rate of CARB into B during night time, and with the rate of CARB synthesis during day time.

**Table 1. Optimal objective values**

Constraint ( $\mu\text{M}\cdot\text{h}^{-1}\cdot\mu\text{MB}^{-1}$ )	Objective value ( $\text{mMB}\cdot\text{j}^{-1}$ )	% of best objective value
None	4.128	1
$v_B \leq 0.06$	3.957	95.9
$v_B \leq 0.03$	3.782	91.6
$v_B \leq 0.028$	3.758	91.0
$v_B \leq 0.025$	3.713	90.0

For smaller values of  $v_B$  (Fig 3 red curve), the system may no longer reach a steady-state before day time. This is due to the fact that  $v_B$  has a low enough value to prevent the CARB pool to reach its minimal admissible quota, as dictated by light availability during day time. Like in previous simulations, light replenishes the CARB pool during day time (periodicity constraint (2.8)) and the variations in total carbon biomass  $X$  are consistent with the rate conversion of CARB into B during night time, and with the rate of CARB synthesis during day time.

The experimental data in Lacour et al (2012) suggest that certain microalgae species satisfy a maximal rate of biomass synthesis (Fig 3A). These data also suggest that the maximal rate  $v_B$  might evolve so that the CARB pool nearly reaches its minimal admissible quota value (dictated by light availability during day time) at the end of the dark period (Fig 2, light blue curve). This observation supports the theory stipulating that starch turnover in photosynthetic organisms is regulated so that it is almost, but not completely, exhausted at the end of the dark period (Stitt & Zeeman 2012). It is also interesting to note that such a behavior results in a productivity loss of about 9% only compared with the optimal productivity in the absence of rate limiting constraints.

On imposing a maximal rate constraint on the nitrate assimilation rate ( $v_{NO_3} \leq v_{max}$ ) and on the carbohydrate consumption rate ( $v_{CARB} \leq v_{max}$ ), similar results are obtained: a constraint is mandatory to reproduce the experimental data by Lacour et al. (2012), and the value of the maximal rate is such that the CARB pool nearly reaches its minimal admissible quota at the end of the dark period. This symmetry between the rate limiting constraints suggests that the activities of different enzymes might become synchronized with each other by evolution pressure. The advantage of such a synchronization could be to minimize the accumulation of intermediate metabolites, besides carbon storage molecules, inside the cells.

An inherent advantage of metabolic modelling is that both the intracellular (metabolic fluxes) and macroscopic (substrate

consumption, biomass production) processes can be predicted simultaneously. Although our main focus in this paper has been on macroscopic processes, it is found that the metabolic fluxes predicted by the solution of (8) with maximal rate constraints  $v_B \leq 0.028 \mu\text{M}\cdot\text{h}^{-1}\cdot\mu\text{MB}^{-1}$  are also consistent with available predictions at the macroscopic and metabolic levels (Baroukh et al. 2015b). The dark period is characterized by a heterotrophic-like metabolism, with consumption of carbohydrates, glycolysis in the downward direction and a high respiration rate (Fig 4). During day time, the metabolism is autotrophic-like, characterized by high fluxes in the photosynthesis pathway, and a relative decrease in the magnitude of various other fluxes; upper glycolysis occurs in the glyconeogenic direction to produce the carbohydrates and sugar precursor metabolites (PEP, G6P, R5P) that are necessary for growth. Finally, near the beginning of day time ( $t=12-15\text{h}$ ), the metabolism is mixotrophic-like, namely a mix between autotrophy-like and heterotrophy-like metabolisms, as light is not intense enough yet to meet the carbon and energy growth demands, which are palliated by carbohydrate consumption.

#### 4. CONCLUSION

In this paper, we have presented a DFBA generic model of microalgae under a diurnal light cycle. In order to account for carbon storage, we have adapted the dFBA framework by separating the pool of intracellular metabolites into two categories: those metabolites following a classical QSSA ( $C$ ) and those subject to accumulation ( $A$ ). Our main assumption here is that microalgae can adapt their metabolism in order to optimize functional biomass production (proteins, membrane lipids, DNA, RNA) over a diurnal cycle. Moreover, for improved numerical tractability, we have reduced the optimization problem by exploiting the right kernel of the stoichiometric matrix, and transformed into an LP by discretizing the differential equations using orthogonal collocation.

Several maximal rate constraint scenarios have been tested, which concur to show that the experimentally observed pattern of accumulating carbon storage molecules during day time, followed by their depletion during night time is an optimal strategy. However, a constraint on maximal synthesis rate of functional biomass must be added to reflect biological observations. A constraint on maximal carbohydrate consumption rate or a constraint on nitrate assimilation rate has been shown to be equivalent. Finally, light availability during the day has been shown to determine how much carbon is stored.

Future work will consist in implementing other carbon storage molecules in the model (lipids, glycerol, cyanophycin, ...) to study the impact of the nature of the storage molecule on the dynamic behaviour of the metabolism and on the quantity stored. Implementation of several carbon storage molecules and addition of isodensity constraints or maximal cell volume will also be tested, to study whether these constraints could explain the repartition between several carbon storage molecules. Experimental validation on several species of microalgae will also be considered.

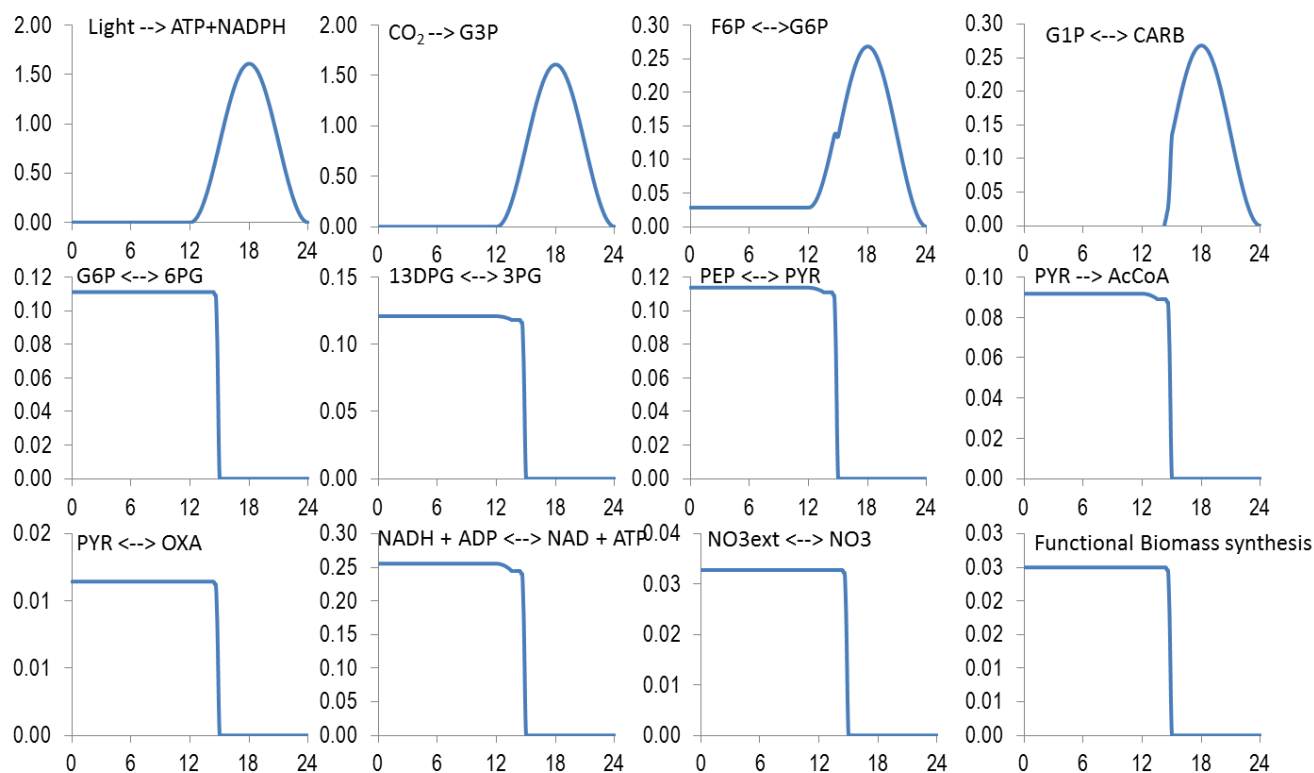


Fig. 4. Metabolic fluxes prediction of the optimization model (2) subject to the maximal rate constraint  $v_B \leq 0.028 \mu\text{M}\cdot\text{h}^{-1}\cdot\mu\text{MB}^{-1}$ . X-axis: Time (h). Y-axis: Fluxes value ( $\mu\text{M}\cdot\text{h}^{-1}\cdot\mu\text{MB}^{-1}$ ).

## REFERENCES

- Baroukh, C. et al., 2014. DRUM: A New Framework for Metabolic Modeling under Non- Balanced Growth. Application to the Carbon Metabolism of Unicellular Microalgae. A. Vertes, ed. PloS one, 9(8), p.e104499.
- Baroukh, C., et al., 2015a. A state of the art of metabolic networks of unicellular microalgae and cyanobacteria for biofuel production. *Metabolic Engineering*, 30, pp.49–60.
- Baroukh, C. et al., 2015b. Mathematical modeling of unicellular microalgae and cyanobacteria metabolism for biofuel production. *Current opinion in biotechnology*, 33, pp.198–205.
- Biegler, L.T., 2010. *Nonlinear Programming: Concepts, Algorithms, and Applications to Chemical Processes*. MOS-SIAM Series on Optimization.
- Bro, C. et al., 2006. In silico aided metabolic engineering of *Saccharomyces cerevisiae* for improved bioethanol production. *Metabolic engineering*, 8(2), pp.102–111.
- Hamilton, J.J. & Reed, J.L., 2013. Software platforms to facilitate reconstructing genome-scale metabolic networks. *Environmental microbiology*, 16(1), pp.49–59.
- Knoop, H. et al., 2013. Flux Balance Analysis of Cyanobacterial Metabolism: The Metabolic Network of *Synechocystis* sp. PCC 6803 C. V. Rao, ed. PLoS Computational Biology, 9(6), pp.1–15.
- Lacour, T. et al., 2012. Diel Variations of Carbohydrates and Neutral Lipids in Nitrogen-Sufficient and Nitrogen-Starved Cyclostat Cultures of *Isochrysis* Sp. *Journal of Phycology*, 48(4), pp.966–975.
- Mahadevan, R., Edwards, J.S. & Doyle, F.J., 2002. Dynamic flux balance analysis of diauxic growth in *Escherichia coli*. *Biophysical journal*, 83(3), pp.1331–1340.
- Mahadevan, R. & Schilling, C.H., 2003. The effects of alternate optimal solutions in constraint-based genome-scale metabolic models. *Metabolic Engineering*, 5(4), pp.264–276.
- Mata, T.M., Martins, A.A. & Caetano, N.S., 2010. Microalgae for biodiesel production and other applications: A review. *Renewable and Sustainable Energy Reviews*, 14(1), pp.217–232.
- Orth, J., Thiele, I. & Palsson, B., 2010. What is flux balance analysis? *Nature biotechnology*, 28(3), pp.245–248.
- Stitt, M. & Zeeman, S.C., 2012. Starch turnover: pathways, regulation and role in growth. *Current opinion in plant biology*, 15(3), pp.282–92.